Z. Phys. C 62, 397–411 (1994)

ZEITSCHRIFT
FÜR PHYSIK C

Optimal observables for the measurement of three gauge boson couplings in $e^+e^- \to W^+W^-$

M.Diehl*, O. Nachtmann

Institut für Theoretische Physik, Universität Heidelberg, Philosophenweg 16, D-69120 Heidelberg, Germany

Received: 1 November 1993

Abstract. We investigate the prospects of measuring anomalous couplings between gauge bosons at electron–positron–colliders with optimal observables. Such observables are shown to contain all information on the coupling parameters that can be extracted in a given reaction. Their sensitivity to the form factors in the general expressions of the triple gauge vertices WWZ and $WW\gamma$, including CP violating terms and absorptive parts, is calculated in view of LEP2 and the NLC.

1 Introduction

The standard model of electroweak interactions has been extensively tested to a high precision in the last years, and has been found in good agreement with the experimental data. One of its features that has not yet been checked by direct measurements is the self-coupling of the weak gauge bosons, whose form in the standard model is completely determined by the local $SU(2) \times U(1)_Y$ symmetry and its breaking in the Higgs sector. With the production of W^+W^- pairs at high energy colliders it will be possible to study the triple gauge vertex between two charged and a neutral vector boson at tree level. At present, the parameters of this coupling are not very much restricted, neither by unitarity [1], nor by indirect bounds from processes where a three boson vertex appears in radiative corrections [2, 3], nor by direct bounds obtained in $p\bar{p}$ collisions [4]. Only for the CP violating part of the coupling some stricter limits have been calculated from their contribution to the electric dipole moments of fermions [3].

A possible way to determine or to restrict coupling parameters is to measure the mean values of observables depending on the momenta of the detected particles. This method has for example been proposed to search for CP violation in Z decays [5, 6] and was shown to be feasible in experimental analyses [7]. An important aspect of integrated observables is that they allow to separate easily couplings with different properties under discrete symmetry transformations, e.g. they can give a clear signal of CP violation under the condition that the experimental setup respects this symmetry.

As was shown in [8], for any coupling or other physical parameter there is an observable which minimises the statistical error in its measurement. This kind of observable has been used for the measurement of the τ polarisation in Z decays [9, 10], where a fit of its distribution was performed. We shall study optimal integrated observables for the detection of anomalous couplings between a neutral and two charged gauge bosons in the reaction $e^+e^- \to W^+W^-$. This will be an issue of interest at LEP2 and a next linear collider NLC, which is under discussion [11].

Our paper is organised as follows. In Sect. 2 we recall some facts about the reaction and the vertex under study, and give the framework of our calculations. We then turn to integrated observables in Sect. 3, discuss relevant symmetry properties, and give some examples for simple observables one can construct. Section 4 deals with general properties of optimal observables as introduced in [8]. Some details about the optimal observables for the process we are investigating are given in Sect. 5. Finally, we present our numerical results and draw conclusions. A proof of the main theorem used in Sect. 4 can be found in the appendix.

2 The reaction $e^+e^- \to W^+W^-$ and the three gauge boson vertices

A reaction suitable for studying the triple gauge vertices WWZ and $WW\gamma$ is W pair production at e^+e^--colliders. At tree level it takes place by annihilation of e^+e^- into a virtual Z or γ which subsequently decays into W^+W^-, or via t-channel exchange of a neutrino (cf. Fig. 1). Experimentally, only hadronic jets or charged leptons from the decay of the Ws can be detected. The mean decay length of

* Supported in part by BMFT, grant no. 05 6HD 93P (6). Address after September 1993: DAMTP, Silver Street, GB-Cambridge CB3 9EW (e-mail: M.Diehl@amtp.cam.ac.uk)

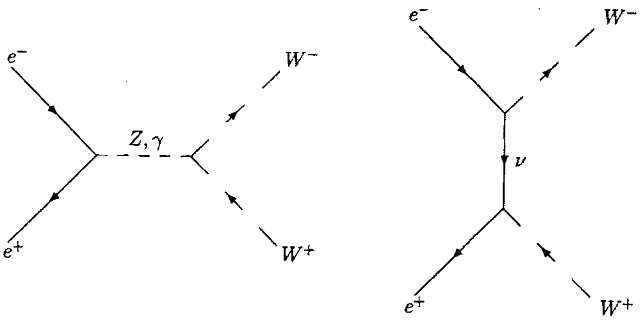

Fig. 1. Tree level Feynman diagrams for $e^+e^- \to W^+W^-$

τ leptons being small (not more than 4 mm at LEP2 energies and smaller than 12.5 mm at $\sqrt{s}=500$ GeV), they cannot be treated on the same footing as the light leptons as far as detection and reconstruction are concerned. Furthermore, events with both W bosons decaying into electrons or muons are disfavoured by their small branching ratio. We shall concentrate on 'semileptonic' events with one W decaying into e or μ and the other into the dijet.

With unpolarised beams and an integrated luminosity of 500 pb^{-1} at LEP2, a run at $\sqrt{s}=190$ GeV, where the total cross section assumes its maximum of about 20 pb, will yield 10 000 W pairs, i.e. 3000 semileptonic events. We also performed calculations at other energies, namely 175 GeV, 180 GeV, and 210 GeV, where the cross section is still above 18 pb. A 500 GeV linear collider NLC with unpolarised beams and 10 fb^{-1} [11] would produce about 75 000 W pairs, the gain in luminosity being much larger than the drop of the cross section to 7.5 pb.

Effects from higher orders in the standard model and from possible new interactions beyond it will modify the production rates, angular distributions, and polarisations of the W pairs as compared to the tree level predictions obtained from the diagrams of Fig. 1. We will study such modifications that are due to a general ansatz for the WWZ and $WW\gamma$ vertex functions. We use the parametrisations of [12], i.e.

$$\Gamma_V^{\alpha\beta\mu}(q,\bar{q},P)= f_1^V(q-\bar{q})^\mu g^{\alpha\beta}-\frac{f_2^V}{M_W^2}(q-\bar{q})^\mu P^\alpha P^\beta+f_3^V(P^\alpha g^{\mu\beta}-P^\beta g^{\mu\alpha}) + i f_4^V(P^\alpha g^{\mu\beta}+P^\beta g^{\mu\alpha})+i f_5^V \varepsilon^{\mu\alpha\beta\rho}(q-\bar{q})_\rho - f_6^V \varepsilon^{\mu\alpha\beta\rho}P_\rho-\frac{f_7^V}{M_W^2}(q-\bar{q})^\mu \varepsilon^{\alpha\beta\rho\sigma}P_\rho(q-\bar{q})_\sigma, \tag{1}$$

where V denotes a Z or γ. $\Gamma_V^{\alpha\beta\mu}$, as well as momenta and Lorentz indices are defined in Fig. 2. The global constants are chosen as

$$g_{WW\gamma}=-e,\ g_{WWZ}=-e\cot\vartheta_W \tag{2}$$

with the positron charge e, and ε is the totally antisymmetric tensor with $\varepsilon_{0123}=1$. The set of f_i^V describes any coupling between on-shell Ws and a Z or γ whose scalar component can be neglected (which is the case for our reaction because, up to terms suppressed by the electron mass, the initial e^+e^--current is conserved). Their relation

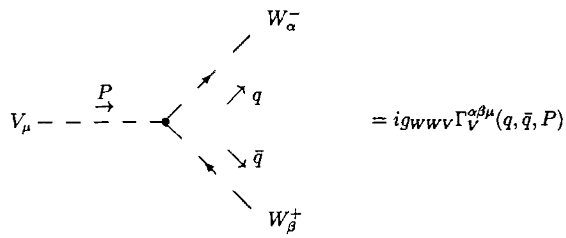

Fig. 2. The triple gauge vertex WWV

with the parameters κ, λ, $\tilde{\kappa}$, $\tilde{\lambda}$ etc. in the effective Lagrangian of the coupling, which are often employed in the literature, can be found in [12]. The couplings with the form factors f_1^V, f_2^V, f_3^V and f_5^V are CP conserving, those with f_4^V, f_6^V and f_7^V CP violating. In our analysis, we shall assume the f_i^V to be complex, their imaginary parts being connected with the absorptive part of the vertex.

At tree level, the standard model predicts $f_1^Z=f_1^\gamma=1$, $f_3^Z=f_3^\gamma=2$ and zero for all other form factors. Since (1) gives the *full* vertex function, the f_i^V obtain contributions from radiative corrections already within the standard model. For simplicity, we call "anomalous" any deviation from the tree level values. In this sense anomalous couplings are not necessarily a sign of new physics. At least for the couplings which are odd under a CP transformation, one can expect a very small contribution from the standard model, where in the present reaction CP violation enters only at two loop level.

For our calculations, we used the coordinate system introduced in [12], p. 270, where the kinematics is described in terms of the angle between the e^- and the W^- in the centre of mass of the e^+e^- annihilation and polar coordinates for the decay products of the Ws in the respective W rest frames. In total there are five angles to consider, not counting the azimuthal angle of the W^-, which enters if detection or experimental cuts violate the rotation symmetry with respect to the beam axis.

We calculated the Born level amplitudes for W production and decay in the helicity basis, with (1) for the three boson couplings and the standard model expressions for all other vertices. One can of course not rule out nonstandard effects which do not originate in the three gauge boson vertices. For a systematic study of all possible anomalous couplings in $e^+e^- \to W^+W^-$ we refer to [13]. For the W propagators, the narrow width approximation was used, and the finite Z width, as well as fermion masses, were neglected. Our phase conventions for spinors are those of [12], and our results for the amplitudes agree with theirs.

The particular choice of phase space coordinates leads to relatively simple expressions for the amplitudes, especially for the terms multiplied by the anomalous parts of the form factors. Namely, the full amplitude is a trigonometric polynomial of first degree in the five angles mentioned above, except for the standard model part, where due to the t-channel neutrino exchange the dependence on the angle θ between e^- and W^- is through a rational function of $\sin\theta$ and $\cos\theta$.

In our numerical calculations, we used the values $M_W=80.22$ GeV and $M_Z=91.17$ GeV [4] and the definition $\sin^2\vartheta_W=1-(M_W/M_Z)^2$ for the weak mixing angle.

For the calculation of the number of events we furthermore took the effective electromagnetic coupling to be $\alpha = 1/128$.

In the reaction we are investigating, both the couplings of the Z and γ are present, and one expects their separation to be difficult. Alternatively, one may work with the linear combinations f_i^L and f_i^R which appear in the amplitudes for left or right handed electrons in the initial state. We define

$$f_i^L = 4\sin^2\vartheta_W f_i^\gamma + (2 - 4\sin^2\vartheta_W)\,\xi f_i^Z$$
$$f_i^R = 4\sin^2\vartheta_W f_i^\gamma - 4\sin^2\vartheta_W\,\xi f_i^Z, \tag{3}$$

where

$$\xi = \frac{s}{s - M_Z^2} \tag{4}$$

is the ratio of the Z and the γ propagators. We shall see that at least for LEP2 energies, the contribution of the f_i^R to the optimal observables can be neglected, which greatly reduces the number of unknown parameters in the analysis.

3 Integrated observables for the detection of anomalous gauge boson couplings

Let us consider the reaction

$$e^+e^- \to W^+W^- \to l^+\nu_l q_d \bar{q}_u, \tag{5}$$

where l stands for e or μ, q_d for a d, s or b quark and q_u for a u or c quark, and write its differential cross section in the form

$$\frac{d\sigma}{d\phi} = S_0 + \sum_i S_{1,i} g_i + \sum_{i,j} S_{2,ij} g_i g_j. \tag{6}$$

Here g_i denotes the real and imaginary parts of the form factors $f_i^{\gamma,Z}$ minus their standard model values at Born level, and ϕ the set of measured phase space variables. The general idea of integrated observables is to choose a function $\mathcal{O}(\phi)$ and to measure its mean value $\langle\mathcal{O}\rangle$. Expressed in a different way, the full distribution of ϕ is weighted with $\mathcal{O}(\phi)$, or it is projected on the distribution of this quantity, and the information about the unknown coupling parameters is then extracted from the mean of this distribution. Neglecting terms of higher order in the presumably small quantities g_i we have

$$\langle\mathcal{O}\rangle = \langle\mathcal{O}\rangle_0 + \sum_i c_i g_i, \tag{7}$$

where $\langle\mathcal{O}\rangle_0$ is the mean value predicted by the standard model. To assess the sensitivity of the observable to anomalous couplings, one further needs the error in the measurement of $\langle\mathcal{O}\rangle$. Its purely statistical part is given by the standard deviation $\Delta\mathcal{O}$ of the distribution of $\mathcal{O}(\phi)$ and the number n of events as $\Delta\mathcal{O}/\sqrt{n}$. The quantity

$$\delta g_i = \frac{1}{|c_i|}\frac{\Delta\mathcal{O}}{\sqrt{n}} \tag{8}$$

is then the absolute value g_i must have so that the mean value $\langle\mathcal{O}\rangle$ differs from the standard model prediction by one standard deviation, assuming the other anomalous couplings to be zero.*

3.1 Discrete symmetries

Let us consider together with (5) the charge conjugated decays of the Ws:

$$e^+e^- \to W^+W^- \to \bar{q}_d q_u l^- \bar{\nu}_l. \tag{9}$$

It is advantageous to define observables $\mathcal{O}^+$ and $\mathcal{O}^-$ of the same dimension for (5) and (9), respectively, and to evaluate the common mean value

$$\langle\mathcal{O}\rangle = \frac{\int d\sigma^+\,\mathcal{O}^+ + \int d\sigma^-\,\mathcal{O}^-}{\int d\sigma^+ + \int d\sigma^-}, \tag{10}$$

where $d\sigma^+$ and $d\sigma^-$ denote the differential cross sections for the respective channels. This not only increases statistics, but, with a judicious choice of $\mathcal{O}^\pm$, also allows to separate different form factors thanks to discrete symmetries, as we shall now see.

We will call an observable CP even if under a CP transformation

$$CP: \mathcal{O}^+ \mapsto \mathcal{O}^-, \tag{11}$$

and CP odd if

$$CP: \mathcal{O}^+ \mapsto -\mathcal{O}^-. \tag{12}$$

We require detector and experimental cuts to be C and P blind, so that the integration domain remains invariant under substitution of the phase space variables with their C and P conjugated ones. Furthermore, we recall that in its centre of mass the initial e^+e^- state is a CP eigenstate for unpolarised beams. Under these circumstances, if an observable is CP odd, its mean value (10) receives no contribution from the CP even terms of the differential cross section. The measurement of a nonzero mean value for a CP odd observable is therefore a clear signal of CP violation in the reaction. Inversely, CP odd terms of the cross section do not contribute to the mean value of a CP even observable.

Our ansatz for $d\sigma/d\phi$ takes all couplings except the one between gauge bosons from the standard model, which in our reaction generates CP violation only at two loop level, and this effect is negligible for our purposes. We do not consider the possibility of anomalous W decays here. Then the only CP odd terms in $d\sigma/d\phi$ come from the interference of a CP violating three boson coupling with the CP conserving part of the $\mathcal{T}$-matrix, and CP even (odd) observables project onto CP even (odd) anomalous boson couplings.

Let us consider next the T and CPT transformation properties of observables. For this, it is essential to distinguish between time reversal T and–following the parlance of [12]–the operation $\tilde{T}$, which reverses particle momenta

---

* The presence of several parameters will be given a more thorough treatment in the next sections

and spins but does not interchange initial and final states. Let $\mathcal{O}$ in (10) be a totally symmetric tensor observable of rank n, where $n=0$ is a scalar, $n=1$ a vector etc.* We will say that $\mathcal{O}$ has a definite $CP\tilde{T}$ parity $\eta_\Theta = \pm 1$, if under a $CP\tilde{T}$ transformation

$$CP\tilde{T}: \mathcal{O}^+ \mapsto \eta_\Theta (-1)^n \mathcal{O}^-. \tag{13}$$

Furthermore, we will always assume CPT invariance to hold. Then an observable of negative η_Θ, when integrated over the whole phase space, can get a nonzero expectation value only if absorptive parts are present in the $\mathcal{T}$-matrix [6, 14]. If cuts are made in phase space, one has to be careful since the initial e^+e^- state gets its momenta reversed by a $CP\tilde{T}$ transformation. Such a reversal of momenta can also be achieved by some rotation R by 180° about an axis perpendicular to the beams. If the cuts are invariant under C, P, $\tilde{T}$, and under a rotation R of the above type, and if

$$R: \mathcal{O}^\pm \mapsto (-1)^n \mathcal{O}^\pm, \tag{14}$$

then it is still true that an observable of negative η_Θ can get a nonzero expectation value only from absorptive parts in the $\mathcal{T}$-matrix.

With the above requirements for the experimental phase space, a term in $d\sigma/d\phi$ will only contribute to the expectation value of an observable $\mathcal{O}$ if it has the same $CP\tilde{T}$ parity η_Θ. In our approximation the only absorptive parts in the $\mathcal{T}$-matrix come from imaginary parts of the form factors f_i^V. Then the expectation value of a $CP\tilde{T}$ odd observable will vanish to zeroth order and a $CP\tilde{T}$ even (odd) observable can have first order contributions only from the real (imaginary) parts of the anomalous form factors.** Of course, beyond tree level, the standard model generates also absorptive parts which are not due to the gauge boson vertex [15].

3.2 Some simple observables

We shall now present some observables constructed with momentum vectors of the W decay products in the laboratory frame. An example for a CP odd tensor observable is defined by setting for $\mathcal{O}^\pm$ in (10)

$$T_{ij}^\pm = (\mathbf{k}_\pm - \mathbf{k}_1)_i (\mathbf{k}_\pm \times \mathbf{k}_1)_j + (\mathbf{k}_\pm - \mathbf{k}_2)_i (\mathbf{k}_\pm \times \mathbf{k}_2)_j + \{i \leftrightarrow j\}. \tag{15}$$

Here $\mathbf{k}_+$ and $\mathbf{k}_-$ denote the momenta of the positive or negative lepton and $\mathbf{k}_1$ and $\mathbf{k}_2$ those of the two jets. Since T_{ij} is symmetric in $\mathbf{k}_1$ and $\mathbf{k}_2$, it is not necessary to distinguish experimentally between the jets. A similar observable can be built with unit momenta:

$$\hat{T}_{ij}^\pm = (\hat{\mathbf{k}}_\pm - \hat{\mathbf{k}}_1)_i \frac{(\hat{\mathbf{k}}_\pm \times \hat{\mathbf{k}}_1)_j}{|\hat{\mathbf{k}}_\pm \times \hat{\mathbf{k}}_1|} + (\hat{\mathbf{k}}_\pm - \hat{\mathbf{k}}_2)_i \frac{(\hat{\mathbf{k}}_\pm \times \hat{\mathbf{k}}_2)_j}{|\hat{\mathbf{k}}_\pm \times \hat{\mathbf{k}}_2|} + \{i \leftrightarrow j\}, \tag{16}$$

and requires only angular measurements in the laboratory frame. Observables of the type (15), (16) have been studied extensively in [5, 6, 14, 16] and have been used by experimentalists to search for CP violation in τ pair production at LEP [7]. If one integrates over the whole phase space in the calculation of $\langle \mathcal{O} \rangle$, it is sufficient to consider only the components T_{33} or $\hat{T}_{33}$, as shown in [6]. The corresponding values δg_i of (8) for the different form factors are given in Table 1 for 190 GeV and 500 GeV c.m. energy. At 190 GeV, one will see a one-standard-deviation-effect if the form factors have a magnitude of some parts in 0.1, the best sensitivity being obtained for f_6^V, whereas for NLC values of 0.02 to 0.04 would already be sufficient.

Changing signs in the definition of the above tensors, one obtains observables U_{ij} and $\hat{U}_{ij}$, which are sensitive to absorptive parts of CP even couplings [14]:

$$U_{ij}^\pm = \pm [(\mathbf{k}_\pm + \mathbf{k}_1)_i (\mathbf{k}_\pm \times \mathbf{k}_1)_j + (\mathbf{k}_\pm + \mathbf{k}_2)_i (\mathbf{k}_\pm \times \mathbf{k}_2)_j + \{i \leftrightarrow j\}], \tag{17}$$

$$\hat{U}_{ij}^\pm = \pm \left[(\hat{\mathbf{k}}_\pm + \hat{\mathbf{k}}_1)_i \frac{(\hat{\mathbf{k}}_\pm \times \hat{\mathbf{k}}_1)_j}{|\hat{\mathbf{k}}_\pm \times \hat{\mathbf{k}}_1|} + (\hat{\mathbf{k}}_\pm + \hat{\mathbf{k}}_2)_i \frac{(\hat{\mathbf{k}}_\pm \times \hat{\mathbf{k}}_2)_j}{|\hat{\mathbf{k}}_\pm \times \hat{\mathbf{k}}_2|} + \{i \leftrightarrow j\} \right]. \tag{18}$$

Our numerical results for these observables are listed in Table 2. Here, at 190 GeV, imaginary parts of f_1^V or f_3^V would produce visible effects if they were at least between 0.4 and 0.8, and the other form factors are practically unmeasurable. At high energy, the situation is somewhat better, where imaginary parts of some 0.1 would be detectable and f_2^V could be measured at the percent level.

A different set of observables, sensitive to CP even or odd couplings, has been studied in [17]. There, anomalous form factors are required to be at least of the order of 0.2 . . . 0.9 to be visible at 200 GeV, except for f_5^V, which is yet harder to detect. For NLC at 500 GeV, these values are found to decrease to 0.01 . . . 0.04 and even to $5 \cdot 10^{-4}$ for f_2^V. Similar results for both real and imaginary parts of

Table 1. One-standard–deviation-accuracies δg_i of (8) obtainable in the measurement of anomalous form factors with the observables T_{33} (15) and $\hat{T}_{33}$ (16). We assume an integrated luminosity of 500 pb^{-1} for LEP2 and of 10 fb^{-1} for NLC. Errors due to numerical integration are below 15% at 500 GeV and below 5% at 190 GeV

$\mathcal{O}$	$\sqrt{s}$[GeV]	Re f_4^γ	Re f_4^Z	Re f_6^γ	Re f_6^Z	Re f_7^γ	Re f_7^Z
T_{33}	190	>1	0.66	0.17	0.12	>1	0.64
	500	0.029	0.024	0.025	0.020	0.12	0.07
$\hat{T}_{33}$	190	>1	>1	0.18	0.12	0.45	0.28
	500	0.041	0.037	0.035	0.027	0.024	0.021

* Here, tensors are defined with respect to the group of spatial rotations

** This remains true if one does not use the narrow width approximation for the W. At tree level, the finite W width does not contribute to the $CP\tilde{T}$ odd part of $d\sigma/d\phi$, where only squared W propagators occur

Table 2. Same as Table 1, but for the observables U_{33} (17) and $\hat{U}_{33}$ (18). Integration errors are smaller than 20% at 500 GeV and smaller than 10% at 190 GeV

$\mathcal{O}$	$\sqrt{s}$ [GeV]	$\mathrm{Im}\, f_1^\gamma$	$\mathrm{Im}\, f_1^Z$	$\mathrm{Im}\, f_2^\gamma$	$\mathrm{Im}\, f_2^Z$	$\mathrm{Im}\, f_3^\gamma$	$\mathrm{Im}\, f_3^Z$	$\mathrm{Im}\, f_5^\gamma$	$\mathrm{Im}\, f_5^Z$
U_{33}	190	0.82	0.43	>1	>1	>1	0.66	>1	>1
	500	0.12	0.097	0.0084	0.0084	0.39	0.24	0.38	>1
$\hat{U}_{33}$	190	>1	0.80	>1	>1	0.72	0.49	>1	>1
	500	0.13	0.11	0.017	0.016	0.13	0.11	0.27	0.15

the couplings have been obtained in [18], where also the decay channels with two leptons were considered.

The authors of [15] proposed the measurement of an asymmetry in lepton–dijet-events, corresponding to an observable which in the channel with a negative decay lepton reads

$$\mathcal{O}^- = \mathrm{sign}(\mathbf{k}_- \cdot (\mathbf{k}_{\mathrm{jetmax}} \times \mathbf{k}_{\mathrm{jetmin}})), \tag{19}$$

where by definition $|\mathbf{k}_{\mathrm{jetmax}}| > |\mathbf{k}_{\mathrm{jetmin}}|$. We are, however, not able to reproduce their numerical results. In both their and our calculation, this asymmetry receives no contribution from f_7^Y, which we also checked analytically. At $\sqrt{s} = 200$ GeV, we find for the asymmetry

$$\langle \mathcal{O}^- \rangle = \mathcal{AS}^{\mathrm{jetmax/jetmin}} = -0.0049(1) f_6^\gamma - 0.0074(2) f_6^Z, \tag{20}$$

where we have indicated numerical integration errors (90% C.L.) in parentheses. In [15] a different parametrisation of the three gauge boson vertex is used, which is related to ours through

$$f_6^\gamma = \delta^\gamma + \cos^2\vartheta_W \hat{\delta}^\gamma, \quad f_7^\gamma = \tfrac{1}{2}\cos^2\vartheta_W \hat{\delta}^\gamma$$
$$f_6^Z = \frac{\delta^Z}{\cos^2\vartheta_W} + \hat{\delta}^Z, \quad f_7^Z = \tfrac{1}{2}\hat{\delta}^Z, \tag{21}$$

assuming that the charge e is taken as positive in [15]. With these parameters our result (20) reads

$$\mathcal{AS}^{\mathrm{jetmax/jetmin}} = -0.0049\delta^\gamma - 0.0096\delta^Z - 0.0038\hat{\delta}^\gamma - 0.0074\hat{\delta}^Z, \tag{22}$$

whereas in [15] (bottom of p. 582) one finds

$$\mathcal{AS}^{\mathrm{jetmax/jetmin}} = 0.31\delta^\gamma + 0.62\delta^Z + 0.24\hat{\delta}^\gamma + 0.48\hat{\delta}^Z, \tag{23}$$

which is roughly a global factor of 65 larger and differs by the global sign. Comparison at different $\sqrt{s}$ (cf. Table 7 of [15]) shows this factor to behave like s. Assuming $n = 3000$ semileptonic events, an asymmetry can be measured to a precision of $1/\sqrt{n} = 0.018$, so that with our values (20), (22), this observable is rather insensitive to anomalous couplings.

4 Optimal observables

We wish to treat the general problem of measuring the value of a physical parameter g in a reaction where it gives a small contribution to the differential cross section. We require that it be possible to work with a power series expansion in g and keep only the leading nontrivial terms. One way to determine g is by the measurement of the mean value of an appropriate observable. The authors of [8] gave the general expression of the observable for which the statistical error in the determination of g is minimal. In [9] it was shown in a somewhat different context that this observable contains the full information on g in the given reaction. We will extend the argument to several unknown parameters and pay special attention to the case where for $g = 0$ the observable has a nonvanishing expectation value.

The results of an experiment which measures a specified set of phase space variables (momenta or polarisations) for a number of events can be characterised by a random variable x with a probability density $F(x, g_i)$ depending on the parameters $g_i (i = 1 \ldots m)$. The parameters should be independent in the sense that one cannot decrease their number in the amplitude of the reaction by a pure redefinition. An estimation of the g_i is then obtained with a set of functions $\gamma_i(x)$. We will restrict ourselves to unbiased estimators, i.e. require

$$E[\gamma_i] = g_i, \tag{24}$$

where E denotes the expectation value. If there is only one parameter, the uncertainty in the estimation may be measured by the variance of γ. As a generalisation, we consider the ellipsoid in the space of the γ_i which is given by

$$\sum_{i,j} \gamma_i' V(\gamma)^{-1}_{ij} \gamma_j' = 1, \tag{25}$$

where

$$V(\gamma)_{ij} = \mathrm{Cov}(\gamma_i, \gamma_j), \tag{26}$$

is the covariance matrix of the estimators and $\gamma_i' = \gamma_i - g_i$. It is equal to the one-standard-deviation ellipsoid if the γ_i are distributed as a multivariate Gaussian.* One can show (cf. [19]); to make our article self-contained, we give a proof in Appendix A) that for any unbiased estimation this ellipsoid fully contains the ellipsoid given by

$$\sum_{i,j} \gamma_i' I_{ij} \gamma_j' = 1 \tag{27}$$

with the so called information matrix

$$I_{ij} = E\left[\frac{\partial}{\partial g_i} \ln F \frac{\partial}{\partial g_j} \ln F\right]. \tag{28}$$

* As we will see, this is the case if one estimates the g_i from the mean values of observables

In the case of one parameter, this reduces to a lower bound for the variance of the estimator, known as the Rao–Cramér–Fréchet bound [4]. A set of estimators is called *joint efficient* if $V(\gamma)^{-1}=I$, the ellipsoid given by $V(\gamma)^{-1}$ is then the smallest possible, and one may consider the estimation to be optimal.

We will now show that, to lowest order in the g_i, joint efficient estimators can be obtained with appropriately chosen integrated observables. Such observables therefore contain all information about the g_i that can be extracted by *any* method, for instance by a maximum likelihood fit to the measured distributions.*

4.1 Analysis not making use of the total event rate

Let the experiment be carried out with a fixed number n of events, discarding the information contained in the total event rate. Experimentally, the absolute normalisation of the spectra need not be known then. If ϕ_k is the set of measured phase space variables for the k-th event, x is the n-tuple of the ϕ_k and the density function is given by

$$F(\phi_1, \ldots, \phi_n)=\prod_k^n f(\phi_k) \tag{29}$$

with

$$f(\phi)\,\mathrm{d}\phi=\frac{\mathrm{d}\sigma}{\int \mathrm{d}\sigma}. \tag{30}$$

Expanding the differential cross section to first order in g_i

$$\frac{\mathrm{d}\sigma}{\mathrm{d}\phi}=S_0+\sum_i S_{1,i}g_i, \tag{31}$$

straightforward calculation gives, to lowest order,

$$\begin{aligned} b_{ij}&:=E\left[\frac{\partial}{\partial g_i}\ln f\frac{\partial}{\partial g_j}\ln f\right]\\ &=\frac{1}{\int \mathrm{d}\phi S_0}\int \mathrm{d}\phi\,\frac{S_{1,i}S_{1,j}}{S_0}-\frac{\int \mathrm{d}\phi S_{1,i}\int \mathrm{d}\phi\, S_{1,j}}{(\int \mathrm{d}\phi S_0)^2} \end{aligned} \tag{32}$$

and hence

$$I=nb. \tag{33}$$

To determine m parameters g_i, one may choose m observables $\mathcal{O}_i(\phi)$ and measure their mean values

$$\bar{\mathcal{O}}_i=\frac{1}{n}\sum_k^n \mathcal{O}_i(\phi_k) \tag{34}$$

in the same experimental run. Expanding to first order

$$E[\mathcal{O}_i]=E_0[\mathcal{O}_i]+\sum_j c_{ij}g_j, \tag{35}$$

where $E_0[\mathcal{O}_i]$ is the expectation value when all g_i are zero, one has, provided that the coefficient matrix c is nonsingular,

$$g_i=\sum_j c_{ij}^{-1}(E[\mathcal{O}_j]-E_0[\mathcal{O}_j]) \tag{36}$$

and thus an estimator

$$\gamma_i=\sum_j c_{ij}^{-1}(\bar{\mathcal{O}}_j-E_0\,[\mathcal{O}_j]) \tag{37}$$

with $E[\gamma_i]=g_i$ and, in matrix notation,

$$V(\gamma)=\frac{1}{n}c^{-1}\cdot V(\mathcal{O})\cdot(c^{-1})^T, \tag{38}$$

where $V(\mathcal{O})$ is the covariance matrix of the $\mathcal{O}_i$. Expansion in g_i gives

$$\begin{aligned} E[\mathcal{O}_i]&=\frac{\int \mathrm{d}\sigma\mathcal{O}_i}{\int \mathrm{d}\sigma}=\frac{\int \mathrm{d}\phi S_0\mathcal{O}_i}{\int \mathrm{d}\phi S_0}\\ &\quad+\sum_j\left(\frac{\int \mathrm{d}\phi S_{1,j}\mathcal{O}_i}{\int \mathrm{d}\phi S_0}-\frac{\int \mathrm{d}\phi S_0\mathcal{O}_i\int \mathrm{d}\phi S_{1,j}}{(\int \mathrm{d}\phi S_0)^2}\right)g_j, \end{aligned} \tag{39}$$

the expression in large parentheses being c_{ij}, and

$$V(\mathcal{O})_{ij}=\frac{\int \mathrm{d}\phi S_0\mathcal{O}_i\mathcal{O}_j}{\int \mathrm{d}\phi S_0}-\frac{\int \mathrm{d}\phi S_0\mathcal{O}_i\int \mathrm{d}\phi S_0\mathcal{O}_j}{(\int \mathrm{d}\phi S_0)^2}. \tag{40}$$

Since for large n the mean values $\bar{\mathcal{O}}_i$ obey a normal distribution, the estimators γ_i are distributed as a multivariate Gaussian.

For the case of a single parameter, the optimal observable is $\mathcal{O}=S_1/S_0$, as found in [8]. We show now that in generalisation of this the set of optimal observables for the case of m parameters reads

$$\mathcal{O}_i=\frac{S_{1,i}}{S_0}\quad(i=1\ldots m), \tag{41}$$

which intuitively may be regarded as the signal to background ratio in the expansion (31) of the cross section. Indeed, from (39) and (40), one sees that for these observables

$$c=V(\mathcal{O})=b, \tag{42}$$

where b is defined in (32), so that with (38) and (33) we have

$$V(\gamma)^{-1}=nb=I \tag{43}$$

and thus a joint efficient estimation of the g_i.

4.2 Analysis making use of the total event rate

Our previous calculation is valid for both vanishing and nonvanishing $E_0[\mathcal{O}_i]$. In the second case, however, the g_i can give a contribution to $\int \mathrm{d}\sigma$, i.e. to the total event rate. To exploit this additional information, let us assume the experiment to be run for a fixed period of time. The

* In the limit of a large number of events, the maximum likelihood method gives estimators γ_i which are unbiased, obey a multivariate Gaussian distribution, and are joint efficient [19]

expected number n of events follows a Poisson distribution

$$p_n=\frac{E[n]^n}{n!}e^{-E[n]}, \tag{44}$$

with the mean value

$$E[n]=\mathscr{L}\int \mathrm{d}\sigma, \tag{45}$$

where $\mathscr{L}$ is the integrated luminosity. The probability to have n events with coordinates $\phi_1, \ldots, \phi_n$ is

$$\tilde{F}(n, \phi_1, \ldots, \phi_n)\prod_k^n \mathrm{d}\phi_k=p_n\prod_k^n (f(\phi_k)\,\mathrm{d}\phi_k) \tag{46}$$

with f as in (30). An estimator γ_i is now a function of n and the ϕ_k. For the calculation of the information matrix $\tilde{I}$ (28) we need

$$\frac{\partial}{\partial g_i}\ln\tilde{F}=\frac{1}{p_n}\frac{\partial}{\partial g_i}p_n+\sum_k^n\frac{\partial}{\partial g_i}\ln f(\phi_k), \tag{47}$$

where, using that to lowest order

$$\frac{1}{E[n]}\frac{\partial}{\partial g_i}E[n]=\frac{\int \mathrm{d}\phi S_{1,i}}{\int \mathrm{d}\phi S_0}, \tag{48}$$

we rewrite the first term as

$$\frac{1}{p_n}\frac{\partial}{\partial g_i}p_n=\frac{\int \mathrm{d}\phi S_{1,i}}{\int \mathrm{d}\phi S_0}(n-E[n]), \tag{49}$$

and after some manipulation find

$$\tilde{I}=E[n]\,d \tag{50}$$

with

$$\mathrm{d}_{ij}=\frac{1}{\int \mathrm{d}\phi S_0}\int \mathrm{d}\phi\,\frac{S_{1,i}S_{1,j}}{S_0}. \tag{51}$$

The term with $\int \mathrm{d}\phi S_{1,i}\cdot\int \mathrm{d}\phi S_{1,j}/(\int \mathrm{d}\phi\, S_0)^2$ present in the information matrix I of (33) in the previous subsection, has been compensated by the contribution of (49).

The ellipsoid given by the new information matrix $\tilde{I}$ is contained in the one defined by I if one sets equal $E[n]$ and n in their respective expressions (50) and (33). To see this, we write the difference between d and b as

$$a_{ij}:=d_{ij}-b_{ij}=\frac{\int \mathrm{d}\phi S_{1,i}}{\int \mathrm{d}\phi S_0}\cdot\frac{\int \mathrm{d}\phi S_{1,j}}{\int \mathrm{d}\phi S_0}=a_i\cdot a_j \tag{52}$$

with

$$a_i=\frac{\int \mathrm{d}\phi S_{1,i}}{\int \mathrm{d}\phi S_0}, \tag{53}$$

and obtain for an arbitrary vector $\mathbf{u}$ the inequality

$$\mathbf{u}^T b\mathbf{u}=\mathbf{u}^T d\mathbf{u}-\mathbf{u}^T a\mathbf{u}=\mathbf{u}^T d\mathbf{u}-(\sum_i u_i a_i)^2\le\mathbf{u}^T d\mathbf{u}. \tag{54}$$

To have equality for all $\mathbf{u}$, one must require all a_i to be zero. This means that the ellipsoid defined in (27) with $I=nd$ is indeed smaller than the one with $I=nb$ unless all $\int \mathrm{d}\phi S_{1,i}$ vanish, in which case the total event rate carries no information about the g_i. It should however be borne in mind that in real life the estimation described in this subsection will be affected by systematic errors connected with the absolute normalisation.

We now show how a joint efficient estimation with the new information matrix $\tilde{I}$ may be achieved by measurement of the same observables as above, when a modified analysis is performed, which instead of the mean values $\bar{\mathcal{O}}_i$ uses their product with the observed number n of events*

$$n\bar{\mathcal{O}}_i=\sum_k^n\mathcal{O}_i(\phi_k). \tag{55}$$

We have

$$E[n\bar{\mathcal{O}}_i]=E[n]\,E[\mathcal{O}_i]=\mathscr{L}(\int \mathrm{d}\phi S_0\mathcal{O}_i+\sum_j g_j\int \mathrm{d}\phi S_{1,j}\mathcal{O}_i)$$

$$=E_0[n\bar{\mathcal{O}}_i]+\sum_j\tilde{c}_{ij}g_j, \tag{56}$$

where we define

$$\tilde{c}_{ij}=\mathscr{L}\int \mathrm{d}\phi S_{1,j}\mathcal{O}_i. \tag{57}$$

With the optimal observables given by (41), $(\tilde{c}_{ij})$ is a positive definite matrix which, therefore, can be inverted and we get

$$g_i=\sum_j\tilde{c}_{ij}^{-1}(E[n\bar{\mathcal{O}}_j]-E_0[n\bar{\mathcal{O}}_j]). \tag{58}$$

This suggests the new estimators

$$\tilde{\gamma}_i=\sum_j\tilde{c}_{ij}^{-1}(n\bar{\mathcal{O}}_j-E_0[n\bar{\mathcal{O}}_j]). \tag{59}$$

The covariance matrix of the quantities $n\bar{\mathcal{O}}_i$ is found to be

$$\mathrm{Cov}(n\bar{\mathcal{O}}_i, n\bar{\mathcal{O}}_j)=E[n]\,E[\mathcal{O}_i\mathcal{O}_j]=\mathscr{L}\int \mathrm{d}\phi S_0\mathcal{O}_i\mathcal{O}_j, \tag{60}$$

which for our optimal observables (41) is equal to the coefficient matrix $\tilde{c}_{ij}$ (57), so that we obtain from (51), (50)

$$V(\tilde{\gamma})_{ij}^{-1}=\mathscr{L}\int \mathrm{d}\phi\frac{S_{1,i}S_{1,j}}{S_0}=E[n]\,d_{ij}=\tilde{I}_{ij}, \tag{61}$$

q.e.d

4.3 *Effects of phase space cuts*

Some remarks may be made about phase space cuts. Usually, these cuts are applied both to $\mathrm{d}\sigma$ and to the normalisation integral $\int \mathrm{d}\sigma$ in (30).Thus it is clear that in this case our method will give again the optimal observables, but for the information obtainable with the above cuts.

The analysis described in the previous subsection is clearly optimal, given a certain luminosity. Applying cuts one can only lose information and thus the error ellipsoid

---

*Setting $\mathcal{O}=1$, this reduces to the measurement of the total cross section

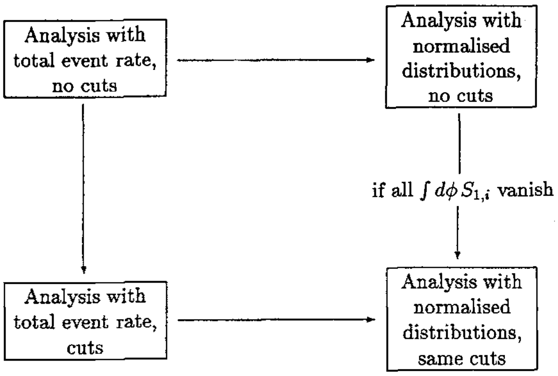

Fig. 3. Different types of analyses with optimal observables. The loss of information and corresponding increase of the error ellipsoid is indicated by arrows

can only become larger. To see this explicitly we use (61) to write (25) of the error ellipsoid as

$$\sum_{i,j} u_i V(\tilde{\gamma})_{ij}^{-1} u_j = \mathscr{L} \sum_i \int \mathrm{d}\phi \frac{(u_i S_{1,i})^2}{S_0} = 1. \tag{62}$$

Applying a cut is tantamount to restricting the domain of integration in the second expression, which can only decrease then. This can be compensated by increasing the length of the vector **u**, so the ellipsoid becomes indeed larger.

Furthermore, one can only lose information when going from the analysis using the total event rate to the one of Subsect. 4.1 using normalised distributions. If an analysis using only normalised distributions is improved or not by imposing cuts can only be decided on general grounds if all $\int \mathrm{d}\phi S_{1,i}$ are zero. As we have seen in Subsect. 4.2, the error ellipsoid is then the same as for the analysis using the total event rate when taking the number of events to be $n = \mathscr{L} \int \mathrm{d}\sigma$, and we can again apply our above argument.*

We have summarised the situation in a diagram (Fig. 3) where we always assume that optimal observables (34), (55) are used.

5 Optimal observables for $e^+e^- \to W^+W^-$

We will now investigate the optimal observables for the measurement of three boson couplings with semileptonic events in $e^+e^- \to W^+W^-$.

If the charge of the parent quarks can be tagged for the jets, the set of optimal observables will be

$$\mathcal{O}_i^{\pm}(\phi) = S_{1,i}^{\pm}(\phi)/S_0^{\pm}(\phi). \tag{63}$$

Here $S_{1,i}^{\pm}$ and $S_0^{\pm}$ are taken from the expansion (31) of the differential cross section $\mathrm{d}\sigma^{\pm}$ for the appropriate W^+W^- decay channel (5) or (9). We would like to emphasise that the phase space variables ϕ can be chosen as any set of coordinates convenient for the experimentalist.*

Without charge tagging, one has experimental information in a reduced phase space. If the W^- decays hadronically, one may for example replace in ϕ the momentum k_d of the d-type quark with the momentum k_1 of the jet with bigger energy in the laboratory frame. The cross section for this modified phase space is the sum of the contributions where the parent quark of this jet is either of d-type ($k_1 = k_d$, $k_2 = k_{\bar{u}}$) or of $\bar{u}$-type ($k_1 = k_{\bar{u}}$, $k_2 = k_d$), denoting by k_2 the momentum of the jet with smaller energy. The optimal observables now read

$$\mathcal{O}_i^+ = \frac{S_{1,i}^+(k_d = k_1) + S_{1,i}^+(k_d = k_2)}{S_0^+(k_d = k_1) + S_0^+(k_d = k_2)}, \tag{64}$$

where the dependence on the other phase space variables is not displayed. Phrased in a different way, one has to sum in the numerator and the denominator of (63) over the expressions obtained when the coordinates of the d-type quark in $S_{1,i}^+$ and S_0^+ are set equal to those of either of the two jets. It is therefore not even necessary to single out one of the jets kinematically. In the same way, the observables $\mathcal{O}_i^-$ for hadronic W^+ decay are constructed, and then $\mathcal{O}_i^+$ and $\mathcal{O}_i^-$ are taken together according to (10). Note that a similar summation allows to write down optimal observables for leptonic decay of both Ws, where one has a different ambiguity in phase space, because due to the escaping neutrinos the kinematics cannot be fully reconstructed [12].

We wish to make a remark concerning the region of forward scattering of the W^- with respect to the e^- direction. At NLC energies one can expect this region of phase space to be affected by experimental cuts, because in the laboratory frame the direction of the W decay products tends to be close to the W direction. In the amplitudes, this region is enhanced by a factor of $1/t$ coming from the neutrino propagator in the t-channel diagram, the effect being considerable at high energy. On the other hand, as $1/t$ appears squared in S_0 but only linear in the interference terms $S_{1,i}$, our optimal observables (63), (64) are *suppressed* by t in the same region. The effect cancels in the integral

$$\int \mathrm{d}\phi \frac{S_{1,i} S_{1,j}}{S_0}. \tag{65}$$

In Subsect. 4.3 we have discussed for which types of analyses this expression determines how the error ellipsoid of the estimators is changed by cuts (cf. (62)). In these cases the loss of information will not be as strong as the loss in the total number of events, if events in this phase space region have to be cut away.

6 Results

Before we discuss our numerical results some remarks are in order about their presentation. In the following we will

---

* In our application of optimal observables to $e^+e^- \to W^+W^-$ we find the terms with $\int \mathrm{d}\phi S_{1,i}$ in the information matrix (33) to be numerically negligible if they are not zero for symmetry reasons (cf. section 6), so that even then one would not expect the sensitivity to be improved by cuts

* A FORTRAN routine with the expressions for the observables in the phase space parametrisation of [12] may be obtained from the authors

always assume that an analysis is made using only normalised distributions, not the total event rate.

In a most simple analysis one takes all anomalous form factors except one to be zero. This parameter can then be estimated from the single measurement of

$$E[\mathcal{O}_i]=E_0[\mathcal{O}_i]+c_{ii}g_i \tag{66}$$

and the standard deviation of this estimation is

$$\delta g_i=\frac{1}{|c_{ii}|}\sqrt{\frac{V(\mathcal{O})_{ii}}{n}}, \tag{67}$$

which we have already used in Sect. 3. If all other g_j are indeed zero, this is an efficient estimate if one uses the optimal observable $S_{1,i}/S_0$, so the quantity δg_i in (67) cannot be smaller for any other observable. In practice, one may assume (66) to hold approximately if for a given i the off-diagonal elements c_{ij} in the full expansion (35) of $E[\mathcal{O}_i]$ are negligible compared to c_{ii}. One can then determine g_i independently of the other form factors, which simplifies the analysis. More generally, if for a subset of the g_i the off-diagonal elements of c with the remaining form factors are negligible, this subset can be analysed independently. We shall see that this is often the case, particularly in the basis of the left and right handed form factors introduced in Sect. 2.

If correlations are important, one needs to consider the full covariance matrix $V(\gamma)$ of the estimators γ_i, which defines the one-standard-deviation ellipsoid (25). Its centre is the origin of the coordinate system with the variables $\gamma_i'=\gamma_i-g_i$, and its intersection with the γ_i'-axis is given by

$$\bar{\delta} g_i=\frac{1}{\sqrt{V(\gamma)_{ii}^{-1}}}. \tag{68}$$

As we have seen in subsection 4.1, for the optimal observables (41) we have $V(\gamma)^{-1}=nb$ and $b=c=V(\mathcal{O})$ (cf. (43) and (42)). In this case $c_{ii}>0$ and therefore

$$\delta g_i=\bar{\delta} g_i=\frac{1}{\sqrt{nc_{ii}}}, \tag{69}$$

i.e. the errors δg_i give also the *intersections* of the full one-standard-deviation ellipsoid with the axes.

The standard deviation of the estimator γ_i in the presence of all other form factors is of course given by

$$\Delta g_i=\sqrt{V(\gamma)_{ii}}. \tag{70}$$

Geometrically this value is obtained by *projection* of the ellipsoid on the corresponding axis. It is evident from Fig. 4 that both δg_i and Δg_i give an imperfect picture of the situation if correlations are large. In this case it would be appropriate to work with linear combinations of form factors for which the correlations are smaller (this is in part realised by the left and right handed combinations of (3)). As shown in Fig. 4 it is rather δg_i than Δg_i that indicates how large the standard deviation is for the combination which can be measured *best*. In this spirit we will use the δg_i in our presentation, but also give the complete

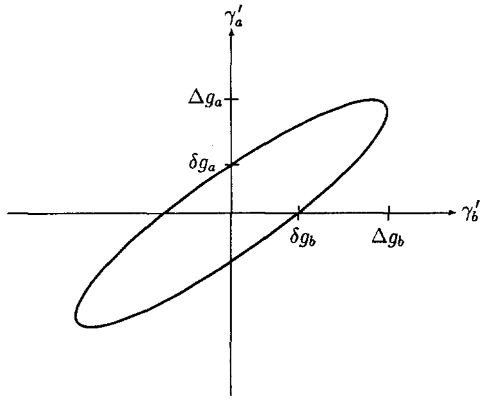

Fig. 4. One-standard–deviation-ellipsis for an estimation with optimal observables in the case of two estimated parameters. δg_i gives the interaction with the γ_i'-axis, Δg_i the projection

covariance matrix $V(\gamma)$ for one case (Table 9). We shall further discuss the correlations between the different observables $\mathcal{O}_i$. They are to be taken from the coefficient matrix c which for optimal observables is equal to the covariance matrix $V(\mathcal{O})$.

Let us now present our results in some detail. For simplicity, we shall only write f_i whenever we want to refer simultaneously to the real and the imaginary parts of f_i^γ and f_i^Z.

At $\sqrt{s}=190$ GeV, we find for most form factors values of δf_i between 0.05 and 0.15 (cf. Table 3). The smallest values are obtained for δf_3, δf_6 and δf_7, whereas for f_5 only a poor resolution can be achieved. In the case of *CP* even form factors, the results are somewhat better for the real than for the imaginary parts, for the *CP* odd ones the opposite is true. The complete coefficient matrix $c=V(\mathcal{O})$ is given in Table 4. By construction of our observables, c is block diagonal, the blocks corresponding to the form factors with the same transformation properties under *CP* and $CP\tilde{T}$, as discussed in Subsect. 3.1. Off-diagonal terms c_{ij} typically have the same order of magnitude as c_{ii} and c_{jj}, most often they are smaller and in no case greater by more than a factor of 2. The off-diagonal terms of f_5 are, however, negligible compared to the diagonal terms of f_1, f_2 and f_3, so that to a good approximation one can determine these last three form factors without considering f_5. Similarly, one may neglect the off-diagonal terms of f_4 when measuring f_6 and f_7.

To see which improvement can be achieved with charge tagging for the jets, we have also calculated the matrix c for the observables (63) without summation over the jet ambiguity. We find that the correlations between different observables are not much changed and that with charge tagging the uncertainties δf_i are smaller by a factor up to 1.8 (except for $\mathrm{Re} f_6^\gamma$ and $\mathrm{Re} f_6^Z$, where one would gain a factor of 2.7 and 2.2 resp., cf. Table 5). This is to be confronted with additional experimental errors and the loss in detection efficiency that would presumably be introduced.

The same calculation allows to assess the sensitivity of an analysis using events where both W decay into electrons or muons. Compared with semileptonic observables with tagging of the quark charge, i.e. full reconstruction,

Table 3. Errors δf_i (67) for optimal observables without charge tagging for the jets. δf_i is the standard deviation in the estimation of f_i if all other anomalous form factors are set to zero. It also gives the intersection of the full one-standard-deviation ellipsoid with the axis corresponding to f_i (cf. Fig. 4). The assumed number of events corresponds to an integrated luminosity of 500 pb^{-1} at LEP2 energies (175 ... 210 GeV) and of 10 fb^{-1} for NLC (500 GeV). Numerical integration errors, estimated by the integration routine RIWIAD, are smaller than 1.5% at 90% C.L.

$\sqrt{s}$ [GeV]	Ref_1^γ	Ref_1^Z	Ref_2^γ	Ref_2^Z	Ref_3^γ	Ref_3^Z	Ref_5^γ	Ref_5^Z
175	0.27	0.17	0.49	0.33	0.12	0.078	0.49	0.28
180	0.22	0.15	0.29	0.20	0.093	0.066	0.36	0.21
190	0.16	0.11	0.13	0.10	0.069	0.052	0.24	0.14
210	0.098	0.082	0.050	0.043	0.048	0.041	0.15	0.093
500	0.0034	0.0045	0.0002	0.0002	0.0029	0.0038	0.015	0.010

$\sqrt{s}$ [GeV]	Imf_1^γ	Imf_1^Z	Imf_2^γ	Imf_2^Z	Imf_3^γ	Imf_3^Z	Imf_5^γ	Imf_5^Z
175	0.29	0.17	0.64	0.38	0.16	0.095	0.59	0.34
180	0.24	0.15	0.38	0.23	0.13	0.079	0.43	0.25
190	0.18	0.11	0.18	0.11	0.099	0.063	0.29	0.17
210	0.13	0.082	0.074	0.049	0.072	0.049	0.19	0.11
500	0.0093	0.0069	0.0005	0.0004	0.0071	0.0055	0.017	0.011

$\sqrt{s}$ [GeV]	Ref_4^γ	Ref_4^Z	Ref_6^γ	Ref_6^Z	Ref_7^γ	Ref_7^Z
175	0.28	0.17	0.15	0.082	0.25	0.15
180	0.23	0.14	0.14	0.078	0.18	0.10
190	0.18	0.11	0.13	0.071	0.11	0.067
210	0.13	0.089	0.11	0.064	0.064	0.040
500	0.015	0.012	0.018	0.012	0.0023	0.0018

$\sqrt{s}$ [GeV]	Imf_4^γ	Imf_4^Z	Imf_6^γ	Imf_6^Z	Imf_7^γ	Imf_7^Z
175	0.21	0.12	0.065	0.039	0.18	0.11
180	0.17	0.11	0.061	0.038	0.13	0.082
190	0.13	0.085	0.057	0.037	0.081	0.053
210	0.10	0.068	0.054	0.036	0.046	0.032
500	0.014	0.010	0.012	0.0094	0.0016	0.0014

Table 4. The coefficient matrix c from (35) for observables without charge tagging for the quark jets at 190 GeV. All matrix elements are to be multiplied with 10^{-3}. As is seen from (35) and (42), an element c_{ij} gives the contribution of a form factor g_j to the expectation value of $\mathcal{O}_i$ and furthermore is the covariance of the observables $\mathcal{O}_i$ and $\mathcal{O}_j$. The matrix c is block diagonal, the blocks corresponding to the form factors with the same transformation properties under CP and $CP\tilde{T}$. **(a)** $CP+$, $CP\tilde{T}+$; **(b)** $CP+$, $CP\tilde{T}-$; **(c)** $CP-$, $CP\tilde{T}+$; **(d)** $CP-$, $CP\tilde{T}-$. We display these four blocks, all other matrix elements are zero. Since c is symmetric, only matrix elements in the diagonal and above or below are listed. The relative errors in numerical integration are not greater than 3%, except for off-diagonal terms with f_5 and f_4, which generally are small, so that relative errors are larger. The absolute errors are however below $0.2 \cdot 10^{-3}$ for off-diagonal terms with f_5 and below $0.4 \cdot 10^{-3}$ for those with f_4

	Ref_1^γ	Ref_1^Z	Ref_2^γ	Ref_2^Z	Ref_3^γ	Ref_3^Z	Ref_5^γ	Ref_5^Z	**(a)**
	14	17	−14	−15	−22	−22	0.71	0.4	Ref_1^γ
		26	−15	−23	−24	−36	0.15	0.32	Ref_1^Z
			19	20	31	29	−1.1	0.29	Ref_2^γ
Imf_1^γ	10			33	31	52	−0.42	0.3	Ref_2^Z
Imf_1^Z	16	27			70	67	−2.1	4.3	Ref_3^γ
Imf_2^γ	−7.3	−11	9.8			121	−1.4	1.3	Ref_3^Z
Imf_2^Z	−11	−20	15	25			5.8	8.3	Ref_5^γ
Imf_3^γ	−9.6	−15	14	22	34			17	Ref_5^Z
Imf_3^Z	−15	−24	22	35	54	85			
Imf_5^γ	0.73	1.5	−0.99	−1.2	−1.3	−2.2	4		
Imf_5^Z	−0.53	−0.54	0.29	1.4	1.8	2.6	6.6	12	
(b)	Imf_1^γ	Imf_1^Z	Imf_2^γ	Imf_2^Z	Imf_3^γ	Imf_3^Z	Imf_5^γ	Imf_5^Z	

	Ref_4^γ	Ref_4^Z	Ref_6^γ	Ref_6^Z	Ref_7^γ	Ref_7^Z	**(c)**
	10	16	2.8	8.4	−0.01	2.6	Ref_4^γ
		26	5.1	16	−0.46	3.1	Ref_4^Z
			20	33	5.4	10	Ref_6^γ
Imf_4^γ	19			67	12	25	Ref_6^Z
Imf_4^Z	26	47			26	42	Ref_7^γ
Imf_6^γ	1.9	−5.8	103			75	Ref_7^Z
Imf_6^Z	−5.9	−12	145	248			
Imf_7^γ	0.5	−0.44	45	64	51		
Imf_7^Z	−3.5	−6.5	66	107	74	117	
(d)	Imf_4^γ	Imf_4^Z	Imf_6^γ	Imf_6^Z	Imf_7^γ	Imf_7^Z	

Table 5. Same as table 3, but for observables with charge tagging at 190 GeV

$\mathrm{Re}f_1^\gamma$	$\mathrm{Re}f_1^Z$	$\mathrm{Re}f_2^\gamma$	$\mathrm{Re}f_2^Z$	$\mathrm{Re}f_3^\gamma$	$\mathrm{Re}f_3^Z$	$\mathrm{Re}f_5^\gamma$	$\mathrm{Re}f_5^Z$
0.11	0.075	0.11	0.075	0.057	0.041	0.19	0.12

$\mathrm{Im}f_1^\gamma$	$\mathrm{Im}f_1^Z$	$\mathrm{Im}f_2^\gamma$	$\mathrm{Im}f_2^Z$	$\mathrm{Im}f_3^\gamma$	$\mathrm{Im}f_3^Z$	$\mathrm{Im}f_5^\gamma$	$\mathrm{Im}f_5^Z$
0.11	0.067	0.11	0.073	0.068	0.043	0.21	0.12

$\mathrm{Re}f_4^\gamma$	$\mathrm{Re}f_4^Z$	$\mathrm{Re}f_6^\gamma$	$\mathrm{Re}f_6^Z$	$\mathrm{Re}f_7^\gamma$	$\mathrm{Re}f_7^Z$
0.11	0.069	0.049	0.032	0.060	0.040

$\mathrm{Im}f_4^\gamma$	$\mathrm{Im}f_4^Z$	$\mathrm{Im}f_6^\gamma$	$\mathrm{Im}f_6^Z$	$\mathrm{Im}f_7^\gamma$	$\mathrm{Im}f_7^Z$
0.10	0.062	0.042	0.028	0.057	0.038

the δf_i would be larger by a factor $\sqrt{6}\approx 2.4$ due to the branching ratios, which makes them already worse than the semileptonic ones *without* charge tagging (except for $\mathrm{Re}f_6^\gamma$. Further losses will be introduced by summation over the ambiguity due to incomplete kinematical reconstruction. We conclude that with the use of optimal observables the purely leptonic channels are in theory not as good as those with a lepton and a dijet for the study of anomalous couplings. In practice one will, of course, use all possible channels for such a study, be it only to have a cross check on systematic uncertainties. Clearly, the use of optimal observables should be advantageous anywhere.

At lower energy, the general situation is the same as at 190 GeV, with the uncertainties δf_i at 175 GeV being larger by factors between 1.5 and 2.5 (cf. Tables 3 and 6). This is because near threshold the amplitudes with an intermediate γ or Z are suppressed by the velocity β of the W relative to the ν-exchange diagram of Fig. 1. The statistics is hardly lower than at 190 GeV, as we mentioned in Sect. 2. Exceptions are δf_6, which remains stable, and δf_2 with considerable losses at low energy, which can also be explained with the β-dependence of the corresponding amplitudes (cf. Table 4 of [12]). Note, however, that at 175 GeV f_6 cannot be measured exclusively, the contribution of f_7 not being negligible. As for the *CP* conserving couplings, δf_2 and δf_5 are quite uninteresting at this energy.

Inversely, going from 190 GeV to 210 GeV at LEP2 would increase the sensitivity by a factor which is about 2.4 for f_2 and lies between 1.2 and 1.8 for the other form factors (except for f_6, which again barely changes).

For NLC parameters, one obtains significantly better results (cf. Table 3). Namely, all δf_i are then below 0.02, the best values being achieved for δf_7, δf_3, δf_1 and above all for δf_2, which is now a few parts in 10^{-4}. A part of this improvement is due to the assumed increase in luminosity of NLC over LEP2, which contributes a factor $1/\sqrt{20}\approx 0.2$ to the δf_i. The dominance of f_2 and f_7, whose off-diagonal elements c_{ij} generally are greater than the diagonal elements of other form factors by an order of magnitude, can be understood from the appearance of a factor M_W^{-2} in the vertex function (1), which causes the corresponding amplitudes to grow with a higher power of the momenta (Table 4 of [12]).* One should however not forget that the mass scale M_W has been chosen for convenience, and that in an effective Lagrangian approach

* The gains for δf_7 are not as large as for δf_2, because f_7 contributes to amplitudes with two transverse W and f_2 to the amplitude with two longitudinal ones, which further favours f_2 at high energy

Table 6a–d. Same as Table 4, but for $\sqrt{s}=175$ GeV. Relative errors in numerical integration are not greater than 4%, except for off-diagonal terms with f_5, where *absolute* errors are below $0.05\cdot 10^{-3}$, and off-diagonal terms with f_4, where no absolute error exceeds $0.5\cdot 10^{-3}$

	$\mathrm{Re}f_1^\gamma$	$\mathrm{Re}f_1^Z$	$\mathrm{Re}f_2^\gamma$	$\mathrm{Re}f_2^Z$	$\mathrm{Re}f_3^\gamma$	$\mathrm{Re}f_3^Z$	$\mathrm{Re}f_5^\gamma$	$\mathrm{Re}f_5^Z$	(a)
	5	7.3	−2	−2.7	−7	−8.6	0.15	0.19	$\mathrm{Re}f_1^\gamma$
		12	−2.7	−4.5	−9	−15	0.005	0.11	$\mathrm{Re}f_1^Z$
			1.5	2	5.3	6.4	−0.13	0	$\mathrm{Re}f_2^\gamma$
$\mathrm{Im}f_1^\gamma$	4.3			3.4	6.6	12	−0.04	0.11	$\mathrm{Re}f_2^Z$
$\mathrm{Im}f_1^Z$	7.2	12			27	33	−0.52	1	$\mathrm{Re}f_3^\gamma$
$\mathrm{Im}f_2^\gamma$	−1.3	−2.1	0.92			61	−0.37	0.77	$\mathrm{Re}f_3^Z$
$\mathrm{Im}f_2^Z$	−2.1	−3.8	1.5	2.6			1.5	2.4	$\mathrm{Re}f_5^\gamma$
$\mathrm{Im}f_3^\gamma$	3.4	−5.7	2.8	4.6	15			4.7	$\mathrm{Re}f_5^Z$
$\mathrm{Im}f_3^Z$	−5.6	−9.7	4.6	7.8	25	41			
$\mathrm{Im}f_5^\gamma$	0.15	0.38	−0.12	−0.13	−0.35	−0.58	1.1		
$\mathrm{Im}f_5^Z$	−0.17	−0.15	0.035	0.19	0.49	0.71	1.8	3.3	
(b)	$\mathrm{Im}f_1^\gamma$	$\mathrm{Im}f_1^Z$	$\mathrm{Im}f_2^\gamma$	$\mathrm{Im}f_2^Z$	$\mathrm{Im}f_3^\gamma$	$\mathrm{Im}f_3^Z$	$\mathrm{Im}f_5^\gamma$	$\mathrm{Im}f_5^Z$	

	$\mathrm{Re}f_4^\gamma$	$\mathrm{Re}f_4^Z$	$\mathrm{Re}f_6^\gamma$	$\mathrm{Re}f_6^Z$	$\mathrm{Re}f_7^\gamma$	$\mathrm{Re}f_7^Z$	(c)
	4.6	7.5	1.1	3.8	−0.02	0.71	$\mathrm{Re}f_4^\gamma$
		13	2.1	7.4	−0.085	0.83	$\mathrm{Re}f_4^Z$
			16	27	2.8	5	$\mathrm{Re}f_6^\gamma$
$\mathrm{Im}f_4^\gamma$	8.6			55	5.5	11	$\mathrm{Re}f_6^Z$
$\mathrm{Im}f_4^Z$	13	24			5.7	9.9	$\mathrm{Re}f_7^\gamma$
$\mathrm{Im}f_6^\gamma$	1.0	−2.4	89			18	$\mathrm{Re}f_7^Z$
$\mathrm{Im}f_6^Z$	−2.7	−6.5	139	240			
$\mathrm{Im}f_7^\gamma$	0.21	−0.14	20	32	11		
$\mathrm{Im}f_7^Z$	−0.86	−2	32	54	18	29	
(d)	$\mathrm{Im}f_4^\gamma$	$\mathrm{Im}f_4^Z$	$\mathrm{Im}f_6^\gamma$	$\mathrm{Im}f_6^Z$	$\mathrm{Im}f_7^\gamma$	$\mathrm{Im}f_7^Z$	

a more natural choice would be the scale of new physics responsible for the anomalous couplings, so one might expect these form factors to be smaller than the others if that scale is much larger than M_W.

As a general result we obtain that the uncertainty in the determination of the couplings is less for the f_i^Z than for the corresponding f_i^γ and that off-diagonal terms between them in the matrix c are comparable to the diagonal ones. This can partly be explained by the fact that at low energy the Z channel is enhanced by the ratio ξ (4) of the Z and the γ propagators, which is between 1.3 and 1.4 in the energy range we are investigating, but the effect, although smaller and with exceptions, persists at 500 GeV, where ξ is practically one.

We have also calculated the coefficients c_{ij} and the uncertainties δf_i in the basis of the form factors f_i^L and f_i^R (3), which are the natural ones to use in the reaction we are considering (cf. Tables 7, 8 and 9). At LEP2 energies the values of δf_i^L are very close to those of the corresponding δf_i^γ. The correlations between different left handed form factors are similar to those in the γ-Z basis, except that f_5^L can be obtained independently of all other couplings (but only to a low precision). An important reduction in parameter space is however possible thanks to the fact that, up to few exceptions, the right handed form factors may be ignored for the determination of the left handed ones, as can be seen from the matrix c in this basis (Table 8). The f_i^R themselves are hardly measurable at LEP2 energies (the 'best' sensitivity being obtained with respect to $\mathrm{Re}\, f_3^R$ and $\mathrm{Im}\, f_6^R$).

At 500 GeV, the results for the δf_i^L are again similar to those for their δf_i^γ counterparts, but one can no longer neglect the influence of all f_i^R in their measurement. On the other hand, the values for the δf_i^R are now acceptable, too, being at most some parts in 10^{-2}, and for δf_2^R and δf_7^R they are quite good. Still, the errors in the determination of right handed factors are clearly larger than for their left handed partners, except for the real parts of CP even couplings.

An exclusive measurement of the left or right handed combinations of form factors could of course be performed with longitudinally polarised beams. For left handed e^- and right handed e^+ one would have twice as many events as for unpolarised beams, assuming the same integrated luminosity of $10\,\mathrm{fb}^{-1}$. The values of the δf_i^L turn out to be approximately a factor of 2 smaller than without polarisation. For right handed e^- and left handed e^+ we find a similar sensitivity to the δf_i^R (compared with the δf_i^L for polarised beams, the δf_i^R are smaller by a factor between 1 and 1.5 in most cases, and compared with the δf_i^R for unpolarised beams they are reduced by a factor between 4 and 12), but one would have only about 350 semileptonic W^+W^- decays, and it is questionable whether a satisfactory analysis could be performed with such an event sample.

If the $\int d\phi S_{1,i}$ do not vanish, i.e. for real, CP even form factors, a theoretically better estimation is obtained when instead of measuring mean values of observables one makes additional use of the information contained in the event rate, as we have shown in Sect. 4. We have calculated the matrix d of (51), which replaces b in the information matrix (50) for the modified analysis of our optimal observables. Both at LEP2 and at NLC energies we find that the difference between d_{ij} and c_{ij} is small compared with c_{ij}, normally increasing with energy. Numerically, the values of $|(d_{ij}-c_{ij})/c_{ij}|$ are smaller than 10% and most often not larger than 5%. Exceptions are the off-diagonal terms between f_5 and the other form factors, the deviations do however not exceed 40% unless d_{ij} and c_{ij} are negligibly small anyway. The uncertainties δf_i in the

Table 7. Same as Table 3, but in the basis of the left and right handed form factors defined in (3)

$\sqrt{s}$ [GeV]	$\mathrm{Re} f_1^L$	$\mathrm{Re} f_1^R$	$\mathrm{Re} f_2^L$	$\mathrm{Re} f_2^R$	$\mathrm{Re} f_3^L$	$\mathrm{Re} f_3^R$	$\mathrm{Re} f_5^L$	$\mathrm{Re} f_5^R$
175	0.26	1.3	0.49	1.7	0.12	0.33	0.44	1.7
190	0.15	0.58	0.14	0.38	0.074	0.17	0.22	0.66
500	0.0041	0.0091	0.0002	0.0005	0.0035	0.0070	0.013	0.030

$\sqrt{s}$ [GeV]	$\mathrm{Im} f_1^L$	$\mathrm{Im} f_1^R$	$\mathrm{Im} f_2^L$	$\mathrm{Im} f_2^R$	$\mathrm{Im} f_3^L$	$\mathrm{Im} f_3^R$	$\mathrm{Im} f_5^L$	$\mathrm{Im} f_5^R$
175	0.27	1.8	0.57	5.1	0.14	3.5	0.52	4.7
190	0.16	0.88	0.17	1.1	0.089	1.8	0.25	1.7
500	0.0083	0.035	0.0005	0.0020	0.0064	0.070	0.014	0.054

$\sqrt{s}$ [GeV]	$\mathrm{Re} f_4^L$	$\mathrm{Re} f_4^R$	$\mathrm{Re} f_6^L$	$\mathrm{Re} f_6^R$	$\mathrm{Re} f_7^L$	$\mathrm{Re} f_7^R$
175	0.26	1.7	0.13	0.65	0.22	1.8
190	0.16	0.87	0.11	0.44	0.099	0.61
500	0.014	0.061	0.015	0.049	0.0021	0.012

$\sqrt{s}$ [GeV]	$\mathrm{Im} f_4^L$	$\mathrm{Im} f_4^R$	$\mathrm{Im} f_6^L$	$\mathrm{Im} f_6^R$	$\mathrm{Im} f_7^L$	$\mathrm{Im} f_7^R$
175	0.19	0.89	0.060	0.31	0.17	1.4
190	0.13	0.46	0.053	0.22	0.075	0.49
500	0.013	0.034	0.011	0.034	0.0015	0.0091

Table 8a–d. Same as Table 6, but in the basis of left and right handed form factors. Integration errors are below 5% unless the absolute value of a matrix element is smaller than $0.5 \cdot 10^{-3}$, in which cases the absolute errors do not exceed $0.05 \cdot 10^{-3}$

	$\mathrm{Re}f_1^L$	$\mathrm{Re}f_1^R$	$\mathrm{Re}f_2^L$	$\mathrm{Re}f_2^R$	$\mathrm{Re}f_3^L$	$\mathrm{Re}f_3^R$	$\mathrm{Re}f_5^L$	$\mathrm{Re}f_5^R$	(a)
	5.5	0.17	−2.1	−0.14	−6.9	−0.6	0.085	−0.01	$\mathrm{Re}f_1^L$
		0.21	−0.11	−0.15	−0.36	−0.66	0.07	0.02	$\mathrm{Re}f_1^R$
			1.6	0.085	5.2	0.37	−0.03	−0.065	$\mathrm{Re}f_2^L$
$\mathrm{Im}f_1^L$	5.4			0.13	0.29	0.65	−0.05	−0.03	$\mathrm{Re}f_2^R$
$\mathrm{Im}f_1^R$	−0.045	0.12			27	1.5	0.085	−0.53	$\mathrm{Re}f_3^L$
$\mathrm{Im}f_2^L$	−1.6	0.02	1.1			3.5	0.03	−0.23	$\mathrm{Re}f_3^R$
$\mathrm{Im}f_2^R$	0.03	−0.03	−0.01	0.01			1.9	−0.07	$\mathrm{Re}f_5^L$
$\mathrm{Im}f_3^L$	−4.2	−0.01	3.4	−0.02	18			0.13	$\mathrm{Re}f_5^R$
$\mathrm{Im}f_3^R$	0.02	−0.06	−0.01	0.02	0.005	0.03			
$\mathrm{Im}f_5^L$	0.06	−0.04	−0.02	−0.02	0	0.02	1.4		
$\mathrm{Im}f_5^R$	0.18	0	−0.1	0	−0.42	0	−0.03	0.02	
(b)	$\mathrm{Im}f_1^L$	$\mathrm{Im}f_1^R$	$\mathrm{Im}f_2^L$	$\mathrm{Im}f_2^R$	$\mathrm{Im}f_3^L$	$\mathrm{Im}f_3^R$	$\mathrm{Im}f_5^L$	$\mathrm{Im}f_5^R$	

	$\mathrm{Re}f_4^L$	$\mathrm{Re}f_4^R$	$\mathrm{Re}f_6^L$	$\mathrm{Re}f_6^R$	$\mathrm{Re}f_7^L$	$\mathrm{Re}f_7^R$	(c)
	5.6	−0.02	2.4	−0.92	0.23	−0.26	$\mathrm{Re}f_4^L$
		0.14	−0.21	0.06	0.055	−0.015	$\mathrm{Re}f_4^R$
			21	−1.3	4.2	−0.33	$\mathrm{Re}f_6^L$
$\mathrm{Im}f_4^L$	10			0.87	−0.56	0.19	$\mathrm{Re}f_6^R$
$\mathrm{Im}f_4^R$	−0.06	0.47			7.3	−0.19	$\mathrm{Re}f_7^L$
$\mathrm{Im}f_6^L$	−1.6	1.0	105			0.12	$\mathrm{Re}f_7^R$
$\mathrm{Im}f_6^R$	1.1	0.57	0.46	3.9			
$\mathrm{Im}f_7^L$	−0.32	0.16	24	0.33	13		
$\mathrm{Im}f_7^R$	0.45	0.03	0.095	0.55	0.16	0.2	
(d)	$\mathrm{Im}f_4^L$	$\mathrm{Im}f_4^R$	$\mathrm{Im}f_6^L$	$\mathrm{Im}f_6^R$	$\mathrm{Im}f_7^L$	$\mathrm{Im}f_7^R$	

Table 9a–d. The covariance matrices of (43) for the estimation of anomalous couplings with optimal observables at 175 GeV. Diagonal elements are explicitly written as squares, so that one can directly read standard deviations Δg_i (70). Numerically, this matrix was obtained by inversion of the coefficient matrix c of Table 8 and subsequent division by the number of events. Since some elements of c, especially in the submatrix of right handed couplings, are quite small, the corresponding parts of the inverse are rather affected by integration errors and should not be taken too literally. This explains the negative value for the diagonal element of $\mathrm{Im}f_3^R$

	$\mathrm{Re}f_1^L$	$\mathrm{Re}f_1^R$	$\mathrm{Re}f_2^L$	$\mathrm{Re}f_2^R$	$\mathrm{Re}f_3^L$	$\mathrm{Re}f_3^R$	$\mathrm{Re}f_5^L$	$\mathrm{Re}f_5^R$	(a)
	$(0.36)^2$	0.19	0.17	0.5	0.002	−0.046	0.008	0.11	$\mathrm{Re}f_1^L$
		$(6.7)^2$	−0.43	136	0.11	−17	2	−4.2	$\mathrm{Re}f_1^R$
			$(0.93)^2$	−2	−0.12	0.29	−0.029	0.032	$\mathrm{Re}f_2^L$
$\mathrm{Im}f_1^L$	$(0.34)^2$			$(21)^2$	0.372	−59	7.1	−17	$\mathrm{Re}f_2^R$
$\mathrm{Im}f_1^R$	−0.21	$(3.8)^2$			$(0.2)^2$	−0.045	0.006	0.086	$\mathrm{Re}f_3^L$
$\mathrm{Im}f_2^L$	0.17	−0.13	$(0.99)^2$			$(2.9)^2$	−0.96	2.6	$\mathrm{Re}f_3^R$
$\mathrm{Im}f_2^R$	0.059	33	0.083	$(0.17)^2$			$(0.54)^2$	−0.19	$\mathrm{Re}f_5^L$
$\mathrm{Im}f_3^L$	−0.018	0.15	−0.12	−0.009	$(0.23)^2$			$(2)^2$	$\mathrm{Re}f_5^R$
$\mathrm{Im}f_3^R$	−0.48	7	−0.11	65	0.26	−20			
$\mathrm{Im}f_5^L$	−0.015	0.93	0.023	−0.008	0.014	1.7	$(0.51)^2$		
$\mathrm{Im}f_5^R$	−0.63	5.8	0.81	−0.32	0.65	12	0.93	$(6.4)^2$	
(b)	$\mathrm{Im}f_1^L$	$\mathrm{Im}f_1^R$	$\mathrm{Im}f_2^L$	$\mathrm{Im}f_2^R$	$\mathrm{Im}f_3^L$	$\mathrm{Im}f_3^R$	$\mathrm{Im}f_5^L$	$\mathrm{Im}f_5^R$	

	$\mathrm{Re}f_4^L$	$\mathrm{Re}f_4^R$	$\mathrm{Re}f_6^L$	$\mathrm{Re}f_6^R$	$\mathrm{Re}f_7^L$	$\mathrm{Re}f_7^R$	(c)
	$(0.27)^2$	−0.022	−0.005	0.064	0.007	0.054	$\mathrm{Re}f_4^L$
		$(1.6)^2$	0.028	−0.38	−0.041	0.88	$\mathrm{Re}f_4^R$
			$(0.14)^2$	0.012	−0.01	0.012	$\mathrm{Re}f_6^L$
$\mathrm{Im}f_4^L$	$(0.19)^2$			$(0.84)^2$	0.023	−0.91	$\mathrm{Re}f_6^R$
$\mathrm{Im}f_4^R$	0.009	$(0.96)^2$			$(0.23)^2$	0.031	$\mathrm{Re}f_7^L$
$\mathrm{Im}f_6^L$	0	−0.01	$(0.075)^2$			$(2.1)^2$	$\mathrm{Re}f_7^R$
$\mathrm{Im}f_6^R$	0	−0.18	0.001	$(0.42)^2$			
$\mathrm{Im}f_7^L$	0.001	0.009	−0.01	0.001	$(0.21)^2$		
$\mathrm{Im}f_7^R$	−0.083	0.35	0.003	−0.45	−0.038	$(1.7)^2$	
(d)	$\mathrm{Im}f_4^L$	$\mathrm{Im}f_4^R$	$\mathrm{Im}f_6^L$	$\mathrm{Im}f_6^R$	$\mathrm{Im}f_7^L$	$\mathrm{Im}f_7^R$	

determination of single form factors are not improved by more than 5%, so that the theoretical gain presumably will be too small to compensate additional systematic errors.

A remark should be made about the approximation made throughout our analysis to retain only the lowest order terms of an expansion in the anomalous parts of form factors. An indication of its validity may be taken from the exact expression for the total cross section. At LEP2 energies, both linear and quadratic coefficients in the expansion of $\int d\sigma$ are not greater than 0.1 times the zeroth order value $\int d\phi S_0$, so that, if the anomalous parts of the f_i are not much larger than their respective δf_i, the linear part may be neglected against $\int d\phi S_0$ and the quadratic part against the linear one. Some quadratic terms can however be comparable with those linear contributions which have very small coefficients (which is the case for f_5), so for consistency the latter should be neglected, too. At 500 GeV, linear and quadratic coefficients in $\int d\sigma$ are partly larger than the standard model value by one or two orders of magnitude respectively, or even three orders in the case of quadratic coefficients of f_2. Still, our approximation would not be too bad if f_2 was of the order of some parts in 10^{-4} and the other form factors of some parts in 10^{-2}.

7 Conclusions

In the present paper we have studied integrated observables for the detection of anomalous gauge boson couplings in W pair production at e^+e^--colliders.

As we have shown, in any reaction the most sensitive integrated observables which can be found contain all information about the coupling parameters that can be extracted experimentally, assuming that an expansion to lowest order in these parameters is sufficiently good.

Compared with more simple observables for the measurement of anomalous three boson form factors, the optimal observables show a clear improvement in sensitivity. Furthermore, they present a systematic framework for the estimation of several parameters in the sense that for any coupling there is an observable with maximal sensitivity to it.

Numerically we find that for most of the anomalous form factors values around 0.1 would have a statistically significant effect on these observables for lepton-dijet events at LEP2, assuming 500 pb^{-1} and $\sqrt{s}=190$ GeV. This is compatible with the results of [12] and [20], where various angular distributions and correlations were studied. Charge tagging for the jets would reduce the theoretical errors by a factor of about 1.5. On the other hand, optimal observables for purely leptonic events would lead to weaker bounds on the couplings. As is to be expected from the form of the anomalous amplitudes, the sensitivity is quite dependent on the c.m. energy. It generally decreases by a factor of 2 when one goes to 175 GeV, whereas one would gain a factor of roughly 1.5 when running at 210 GeV. The correlations between form factors f_i^γ and f_i^Z are generally strong and it should be advantageous to use the less correlated form factors f_i^L, f_i^R of (3), which appear in the amplitudes for left and right handed beam electrons. For unpolarised beams we find sensitivity only to the f_i^L, whereas the f_i^R are practically unmeasurable. Thus, one could restrict an analysis to the f_i^L, reducing greatly the number of form factors to be determined.

At NLC, the potential for studies of the three gauge boson vertices is considerably higher. We find that one can expect to measure f_2 to a precision of a few 10^{-4} and all other form factors within some parts in 10^{-2}. Using longitudinally polarised e^- and e^+ beams, the determination of the left handed combinations of form factors would be possible with the accuracy improved by a factor of 2, whereas the measurement of the right handed combinations should be difficult because of the very low statistics.

Acknowledgements. We are grateful to J. Gascon, K. Mönig, M. Pohl, E. de Rafael, and D. Schaile for their interest in our work and for discussions. Particular thanks are due to W. Bernreuther, G. Botz, A. Brandenburg, and P. Overmann for valuable help and advice, and to W. Bernreuther and P. Overmann for reading the manuscript.

Appendix A. The generalised Rao-Cramér-Fréchet bound

In this appendix we derive the generalised Rao-Cramér-Fréchet bound used in Sect. 4.

Let $F(x, g_i)$ be the distribution function of a random variable x and $\gamma_i(x)$ a set of linearly independent estimators for the g_i with

$$E[\gamma_i]=g_i. \tag{71}$$

Differentiating the normalisation condition

$$\int dx\, F(x, g_i)=1 \tag{72}$$

with respect to g_i, one obtains

$$\int dx \frac{\partial}{\partial g_i} F=\int dx\, F \frac{\partial}{\partial g_i} \ln F=E\left[\frac{\partial}{\partial g_i} \ln F\right]=0. \tag{73}$$

Similarly, differentiation of (71) with respect to g_j yields

$$E\left[\gamma_i \frac{\partial}{\partial g_j} \ln F\right]=\delta_{ij}. \tag{74}$$

For arbitrary vectors u_i and v_i one has

$$\begin{aligned}0 &\leq E\left[\left(\sum_i\left\{u_i(\gamma_i-g_i)-v_i \frac{\partial}{\partial g_i} \ln F\right\}\right)^2\right] \\ &=\sum_{i,j}\left\{u_i u_j E[(\gamma_i-g_i)(\gamma_j-g_j)]+v_i v_j E\left[\frac{\partial}{\partial g_i} \ln F \frac{\partial}{\partial g_j} \ln F\right]\right. \\ &\quad \left.-2u_i v_j E\left[(\gamma_i-g_i) \frac{\partial}{\partial g_j} \ln F\right]\right\}.\end{aligned} \tag{75}$$

With (73) and (74) this reduces in marix notation to

$$0 \leq \mathbf{u}^T V \mathbf{u}+\mathbf{v}^T I \mathbf{v}-2\mathbf{u}^T \mathbf{v}, \tag{76}$$

where

$$V_{ij} = \mathrm{Cov}(\gamma_i, \gamma_j)$$

$$I_{ij} = E\left[\frac{\partial}{\partial g_i} \ln F \frac{\partial}{\partial g_j} \ln F\right]. \tag{77}$$

Being a covariance matrix of linearly independent quantities, V is positive in any basis and hence can be inverted. Setting $\mathbf{u} = V^{-1}\mathbf{v}$, (76) becomes

$$\mathbf{v}^T V^{-1} \mathbf{v} \leq \mathbf{v}^T I \mathbf{v}, \tag{78}$$

which implies that the ellipsoid $\mathbf{v}^T V^{-1} \mathbf{v} = 1$ fully contains the one given by $\mathbf{v}^T I \mathbf{v} = 1$.

References

1. U. Baur, D. Zeppenfeld: Phys. Lett. B201 (1988) 383
2. G.L. Kane, J. Vidal, C.-P. Yuan: Phys. Rev. D39, (1989) 2617; F. Boudjema, K. Hagiwara, C. Hamzaoui, K. Numata: Phys. Rev. D43 (1991) 2223; G. Altarelli, R. Barbieri: Phys. Lett. B253 (1991) 161; K. Hagiwara, S. Ishihara, R. Szalapski, D. Zeppenfeld: Phys. Lett. B283 (1992) 353
3. F. Boudjema, C.P. Burges, C. Hamzaoui, J.A. Robinson: Phys. Rev. D43 (1991) 3683; A. de Rújula, M.B. Gavela, O. Pène, F.J. Vegas: Nucl. Phys. B357 (1991) 311
4. Particle Data Group: Phys. Rev. D45 11, II (1992)
5. W. Bernreuther, U. Löw, J.P. Ma, O. Nachtmann: Z. Phys. C43 (1989) 117; W. Bernreuther, O. Nachtmann: Phys. Rev. Lett. 63 (1989) 2787
6. W. Bernreuther, G.W. Botz, O. Nachtmann, P. Overmann: Z. Phys. C52 (1991) 567
7. P.D. Acton et al. (OPAL Coll.): Phys. Lett. B281 (1992) 405; D. Buskulic et al. (ALEPH Coll.): Phys. Lett. B297 (1992) 459
8. D. Atwood, A. Soni: Phys. Rev. D45 (1992) 2405
9. M. Davier, L. Duflot, F. Le Diberder, A. Rougé: Phys. Lett. B306 (1993) 411
10. D. Buskulic et al. (ALEPH Coll.): Z. Phys.C 59 (1993) 369
11. e^+e^--collisions at 500 GeV: the physics potential. Part A. Proceedings of the Workshop–Munich, Annecy, Hamburg, 1991. P.M. Zerwas. (ed.) DESY 92-123A
12. K. Hagiwara, R.D. Peccei, D. Zeppenfeld, K. Hikasa: Nucl. Phys. B282 (1987) 253
13. P. Méry, M. Perrottet, F.M. Renard: Z. Phys. C36 (1987) 249
14. W. Bernreuther, O. Nachtmann: Phys. Lett. B268 (1991) 424
15. A. Bilal, E. Massó, A. de Rújula: Nucl. Phys. B355 (1991) 549
16. W. Bernreuther, U. Löw, J.P. Ma, O. Nachtmann: Z. Phys. C41 (1988) 143; J. Körner, J.P. Ma, R. Münch, O. Nachtmann: Z. Phys. C49 (1991) 447; A. Brandenburg, J.P. Ma, R. Münch, O. Nachtmann: Z. Phys. C51 (1991) 225; W. Bernreuther, O. Nachtmann, P. Overmann, T. Schröder: Nucl. Phys. B388 (1992) 53
17. J.P. Ma: Momentum correlations for testing three vector boson couplings in the Standard Model at LEP. Universität Heidelberg preprint HD-THEP-91-33 (1991)
18. M. Diehl: Zur Untersuchung anomaler Kopplungen zwischen drei Eichbosonen in der Elektron–Positron-Annihilation. Diploma Thesis, Universität Heidelberg, 1993
19. H. Cramér: Mathematical Methods of Statistics. New Jersey: Princeton Univ. Press 1958
20. M. Pundurs: Z. Phys. C52 (1991) 449